

Pyridoxal (thio) Semicarbazone Ligands and Their Fe(III) Complexes as Potential Electrocatalysts for Hydrogen Evolution Reaction

Violeta Jevtovic^{1,*}, Khalaf M. Alenezi¹, Hani El Moll¹, Ashanul Haque¹, Jamal Humaidi¹,
Salma A. Al-Zahrani¹, Dragoslav Vidovic²

¹ Chemistry Department, University Hail, Kingdom of Saudi Arabia,

² School of Chemistry, Monash University, Clayton, Melbourne, Australia.

*E-mail : v.jevtovic@uoh.edu.sa

Received: 16 March 2021 / Accepted: 27 April 2021 / Published: 31 May 2021

A significant requirement for a future hydrogen economy and easily accessible renewable energy is efficient production of hydrogen from aqueous protons by direct solar energy conversion. The synthesis of a catalyst that can facilitate the reaction of hydrogen evolution (HER) is of paramount importance to achieve this overall objective. This study focuses on catalytic activity of pyridoxal-semi (H₂-PLSC) and pyridoxal-thiosemi (H₂-PLTSC) carbazone molecules and their iron complexes Fe(H-PLTSC)(PLTSC)·4H₂O and [Fe(H₂-PLSC)Cl₂(H₂O)]Cl, for electrochemical proton reduction into hydrogen. The free ligands (H₂-PLSC and H₂-PLTSC) were able to electrocatalyze the reduction of proton into hydrogen. Even though, the studied complexes were more catalytically active than the free ligand, this observation provided crucial evidence for the proposed mechanism that involved protonation of the ligand.

Keywords: Pyridoxal-semicarbazone, Pyridoxal-thiosemicarbazone, Iron complexes, electrocatalysis

1. INTRODUCTION

Growing worldwide demand for energy and decreasing fossil fuel supplies are intensifying the need to look for alternative sources of clean and renewable energy. [1]. In our move away from today's hydrocarbon economy, hydrogen, as a main energy carrier, is considered a promising alternative.

Using the Earth's plentiful metals Ni and/or Fe in their active sites, under atmospheric pressure and temperature, the nature completes the conversion of protons and electrons into molecular H₂ (2H⁺ + 2e⁻ → H₂). [2,3]

To substitute the less abundant and high-cost platinum-based materials for catalytic proton reduction, the production of affordable proton reduction catalysts based on Earth-abundant elements [4]

such as Fe [5] Ni [6] Cu [7] and Co [8] is a great scientific challenge and a major step towards sustainable conversion of solar energy.

The distorted octahedral Ni(ii) complex $[\text{Ni}(\text{bztpen})]^{2+}$ (bztpen = N-benzyl-N,N',N'-tris(pyridine-2-ylmethyl)ethylenediamine) are some of the most efficient H_2 evolution homogeneous catalysts designed, showing a very high TON of 308 000 over 60 h electrolysis with an applied potential of -1.25 V vs. SHE[9]. It has recently been shown that the efficiency of metal-containing catalysts can be enhanced by synergy between metal- and ligand-based redox activities [10] For the stabilization of otherwise labile low-oxidation-state metals, the electron-rich and π -back-donating sulfur donor character is favorable, facilitating metal hydride intermediates for the HER. For example, dithiolene complexes are known as biological cofactors,[11] and are involved in bioinorganic processes at the Mo and W oxotransferase catalytic centers [12].

The phosphines ligands are traditionally the ligands of choice for transition metal catalysis and, in particular, for substrate coupling reactions. Since phosphines can often be water- and air-sensitive, a number of attempts have been made to develop catalysts that are stabilized with ligands containing C, N, O, or S donor atoms, such as N-heterocyclic and carbocyclic carbenes, oxazolines, amines, imidazoles, hydrazones, thioureas, amidates. Thiosemicarbazones (TSC) and semicarbazones (SC) certainly fall within this classification, as well.

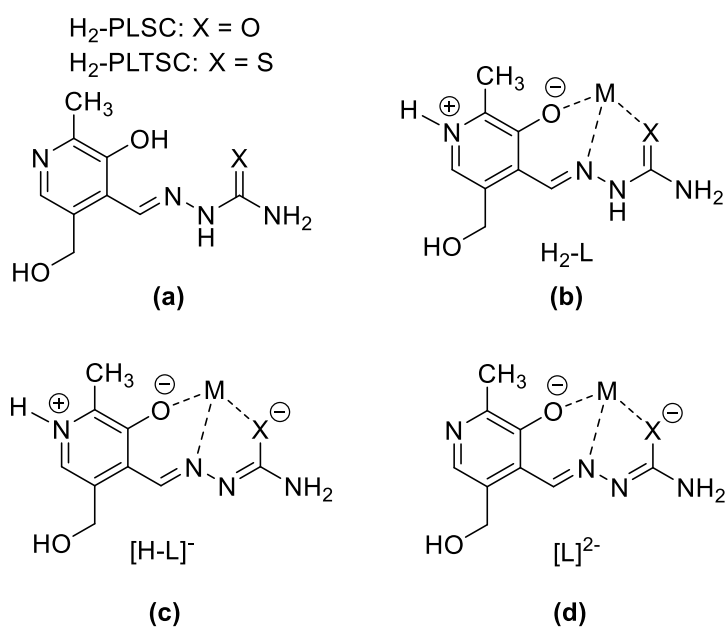


Figure 1. (a) General structure for pyridoxal semicarbazone ($\text{H}_2\text{-PLSC}$) and pyridoxal thiosemicarbazone ($\text{H}_2\text{-PLTSC}$) molecules; (b) neutral ($\text{H}_2\text{-L}$), (c) mono-anionic ($[\text{H-L}]^-$) and (d) di-anionic ($[\text{L}]^{2-}$) coordination modes for these ligands.

The use of thiosemicarbazone or semicarbazone support ligands in catalysis is not relatively new as thiosemicarbazone complexes with transition metals Ru [13, 14], Re [15], Ni [16], Cu [17] and Pd [18] and semicarbazones complexes with Au [15] and Mn [16] as central metal have been reported. Thiosemicarbazones and semicarbazones implementation as ligands in last few decades is a fruitful area

of research as indicated by a Review paper [19] titled: "Thiosemicarbazone Complexes of Transition Metals as Catalysts for Cross-Coupling Reactions", that included detailed mechanistic insights for these reactions.

Recently, ligands based on the semicarbazone and thiosemicarbazone in combination with pyridoxal (form of vitamin B₆) were prepared [20]. Dehydration of SC (full form) or TSC (full form) with pyridoxal moiety (3-hydroxy-5-hydroxymethyl-2-methyl-pyridine-4-carbaldehyde) results in the formation of Schiff base ligands pyridoxal-semicarbazone or pyridoxal-thiosemicarbazone (H₂-PLSC or H₂-PLTSC, Scheme 1), respectively.

H₂-PLSC and H₂-PLTSC are tridentate ligands that normally coordinate to a metal center through phenolic oxygen, hydrazine nitrogen and either oxygen (H₂-PLTS) or sulfur (H₂-PLTSC) atoms. Accordingly, H₂-PLSC is an ONO ligand, while H₂-PLTSC is an ONS ligand. Based on the reported crystallographic characterizations, these ligands are capable of adapting three distinct coordination modes once bound to a transition metal center. The zwitterion form (H₂-L, Figure 1b) is actually a neutral form of the ligands as it is formed by deprotonation of the phenolic OH-group and protonation of the "pyridine" N atom. The monoanionic form ([H-L]⁻, Figure 1c) is obtained through deprotonation of enol/thiol forms, while, the dianionic ([L]²⁻, Figure 1d) form of ligands is obtained through further deprotonation of the pyridine N atom.

As the literature search shows that several transition metals complexes with H₂-PLTSC and H₂-PLSC have been synthesized thus far [20-26]. The complexes have been characterized by classical physicochemical methods, X-ray analysis and biological (anti-bacterial) activities. Transition complexes with these ligands were also used as catalysts [27,28]. Pyridoxal thiosemicarbazone complexes and their recyclable catalytic applications in the nitroaldol (Henry) reaction in ionic liquid media was performed in 2014 [27], while palladium(II) pyridoxal thiosemicarbazone complexes as efficient and recyclable catalyst for the synthesis of propargylamines by a three-component coupling reactions in ionic liquids was reported in 2016 [28].

This research paper focuses on catalytic activities of iron complexes incorporating pyridoxal thiosemicarbazone and pyridoxal semicarbazone ligands, specifically, [Fe(H-PLTSC)(PLTSC)]·4H₂O and [Fe(H₂-PLSC)Cl₂(H₂O)]Cl.

2. EXPERIMENTAL DETAILS

Ligands (H₂-PLSC and H₂-PLTS) and iron complexes were synthesized according to the previously described procedure [20].

Acetic acid (CH₃COOH) was purchased from Aldrich and used as received. Cyclic voltammetry experiments were carried out using an Au-tolab PGSTAT 128 potentiostat. The electrochemical cell containing 5 ml of a solution of electrolyte [NBu₄][BF₄], 0.2 M in DMF, was degassed with nitrogen gas. A conventional three-electrode arrangement was employed, consisting of a vitreous carbon working electrode (CPE) (0.07 cm²), a platinum wire as the auxiliary electrode and Ag/AgCl as a reference electrode.

3. RESULTS AND DISCUSSION

It has been established, via single crystal X-ray diffraction, that $[\text{Fe}(\text{H-PLTSC})(\text{PLTSC})]\cdot 4\text{H}_2\text{O}$ contained one pyridoxal thiosemicarbazone ligand in its mono-anionic ($[\text{H-L}]^-$) form while the other ligand coordinated to the central iron in the di-anionic ($[\text{L}]^{2-}$) form [20]. Nevertheless, complex $[\text{Fe}(\text{H}_2\text{-PLSC})\text{Cl}_2(\text{H}_2\text{O})]\text{Cl}$ contained only one pyridoxal semicarbazone ligand in its neutral ($\text{H}_2\text{-L}$) form [20]. Thus, these complexes, together with the free ligands, were considered adequate candidates for cyclic voltammetry (CV) studies especially with regard to generation of H_2 via proton reduction.

The cyclic voltammetry of $\text{H}_2\text{-PLSC}$ and $\text{H}_2\text{-PLTSC}$ (2.5 mM) were performed in DMF containing 0.2M tetrabutylammonium tetrafluoroborate, $[\text{NBu}_4][\text{BF}_4]$ solution. $\text{H}_2\text{-PLSC}$ ligand exhibit one reduction peak at $E_p^{\text{red}} = -1.45$ V while $\text{H}_2\text{-PLTSC}$ present three non-reversible reduction peaks at E_p^{red} of -0.75 V, -1.0 V and -1.6 V (Fig. 2). For both ligands, it is worth noting that the current varies linearly with the scan rate, with intercept close to zero, indicating a non-complicated mass transfer control (Fig. 3).

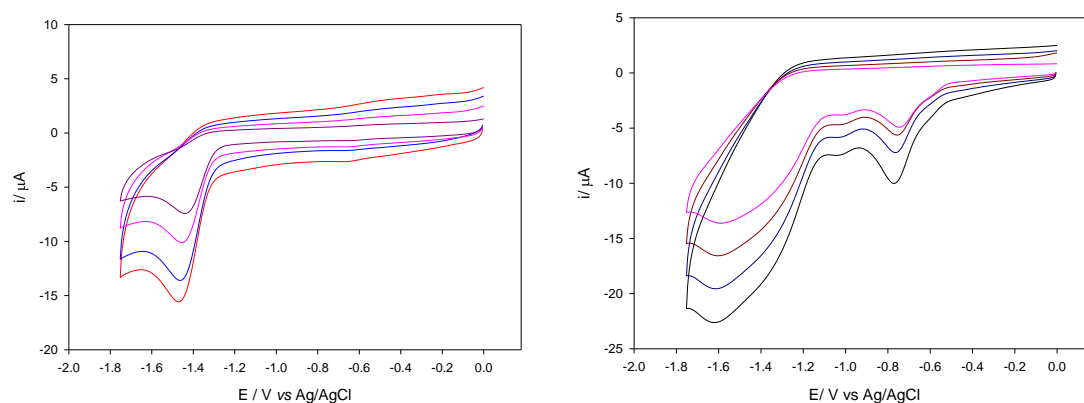


Figure 2. Cyclic voltammetry in 0.2 M $[\text{NBu}_4][\text{BF}_4]$ DMF-solution at carbon electrode with different scan rate under nitrogen of $\text{H}_2\text{-PLSC}$ (left) and $\text{H}_2\text{-PLTSC}$ (right) ligands.

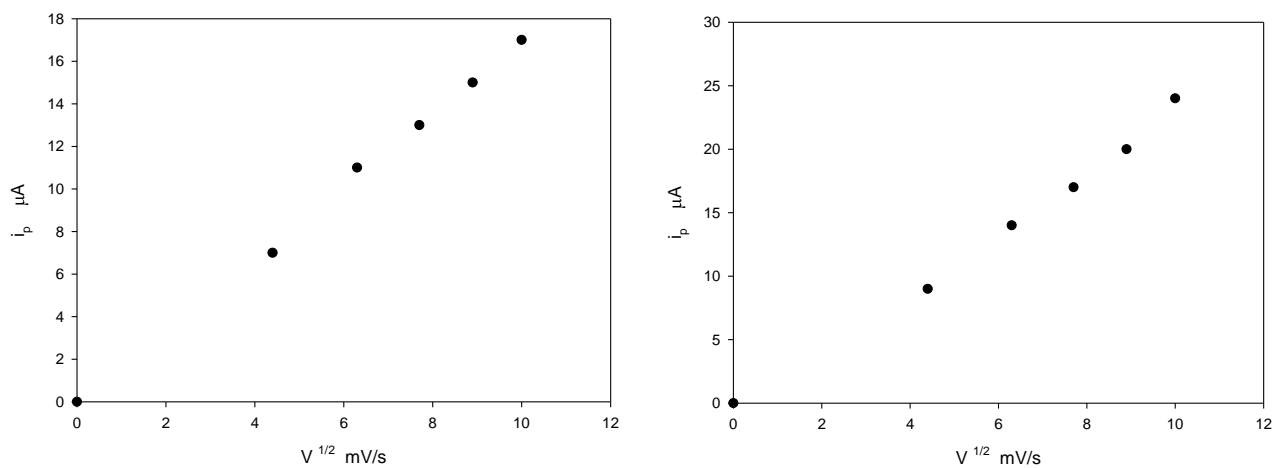


Figure 3. The dependence of square root of the scan-rate ($v^{1/2}$) on the peak current of $\text{H}_2\text{-PLSC}$ (left) and $\text{H}_2\text{-PLTSC}$ (right) ligands (second peak reduction).

The cyclic voltammetry of free-organocatalyst acetic acid (CH_3COOH) in 0.2 M $[\text{NBu}_4][\text{BF}_4]$ -DMF (control experiment) at vitreous carbon electrode were carried out. We note a direct reduction of the acid at $E_p = -1.75 \text{ V vs Ag/AgCl}$. Interestingly, the redox potential E_p shifts, in the presence of PLSC or PLTSC for about 350 mV and 550 mV towards the positive potentials, respectively (Figure 4).

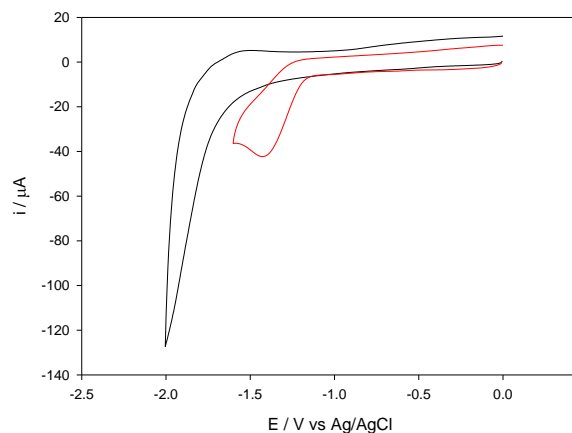


Figure 4. A comparative cyclic voltammetry of the proton reduction of ligand-free, 2.5 mM H_2 -PLSC and 2.5 mM H_2 -PLTSC solutions of acetic acid (CH_3COOH) in $[\text{Bu}_4\text{N}][\text{BF}_4]$ -DMF, scan rate 100 mVs^{-1} at vitreous carbon electrode under N_2 .

In fact, the addition of acetic acid (CH_3COOH) in the presence of H_2 -PLSC or H_2 -PLTSC, provoke the proton reduction process at catalytic currents of -1.4 and -1.2 V vs Ag/AgCl, respectively. This is consistent with the electrocatalytic proton reduction (Figure 5). It is worth noting that the highest electrocatalytic activities are observed in the presence of 2 eq of acetic acid with maximum current 4 time higher than the acid-free medium for both ligands.

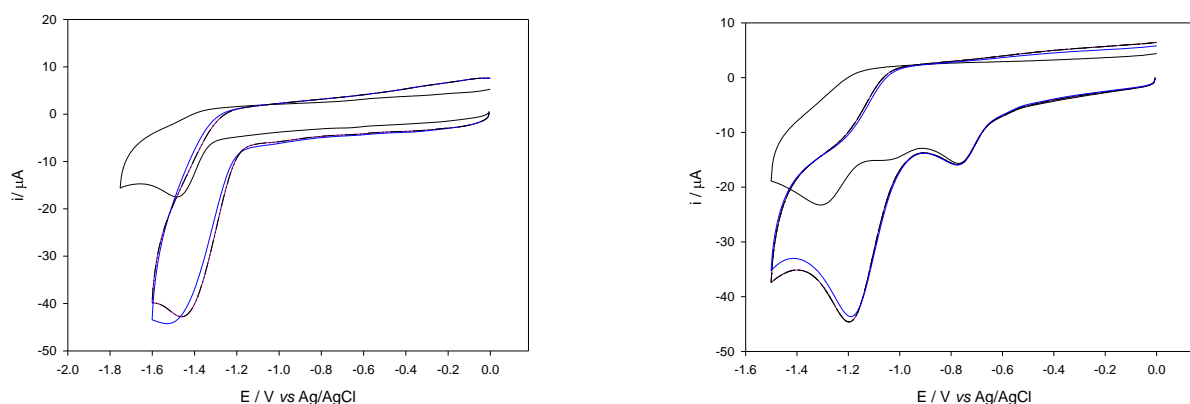


Figure 5. Cyclic voltammetry of 2.5 mM H_2 -PLSC (left) and PLTSC (right) in DMF solutions containing 0.1M $[\text{NBu}_4][\text{BF}_4]$, Rt. Scan rate 100 mVs^{-1} . in presence of 1eq (red), 2 eq (black), 3 eq (blue) of acetic acid at carbon electrode.

The cyclic voltammetry of 2.5 mM DMF solutions of $[\text{Fe}(\text{H}_2\text{-PLSC})\text{Cl}_2(\text{H}_2\text{O})]\text{Cl}$ and $\text{Fe}(\text{H-PLTSC})(\text{PLTSC})\cdot 4\text{H}_2\text{O}$ were performed. These solution contained 0.2M tetrabutylammonium tetrafluoroborate ($[\text{NBu}_4][\text{BF}_4]$) as electrolyte. At negative potentials $[\text{Fe}(\text{H}_2\text{-PLSC})\text{Cl}_2(\text{H}_2\text{O})]\text{Cl}$ exhibits one reduction peak with $E_p^{\text{red}} = -1.5$ V (Figure 6) where $[\text{Fe}(\text{H-PLTSC})(\text{PLTSC})\cdot 4\text{H}_2\text{O}]$ show three reversible reduction peaks at E_p^{red} of -0.75 V, -0.98 V and -1.35 V that correspond to the redox couples $\text{Fe}^{3+}/\text{Fe}^{2+}$, $\text{Fe}^{2+}/\text{Fe}^+$ and Fe^+/Fe^0 respectively (Figure 6). The electrooxidation of the synthesized complexes were studied under the same conditions. In fact, Figure 8 exhibits three peaks that correspond to the oxidation of the ligand. It is worth noting that Figure 6 and Figure 8 show a set of voltammograms recorded at various scan rates for complexes $[\text{Fe}(\text{H}_2\text{-PLSC})\text{Cl}_2(\text{H}_2\text{O})]\text{Cl}$ and $\text{Fe}(\text{H-PLTSC})(\text{PLTSC})\cdot 4\text{H}_2\text{O}$ for both reduction and oxidation processes, respectively. The current varies linearly with the scan rate, with intercept close to zero, indicating a non-complicated mass transfer control Figure 7.

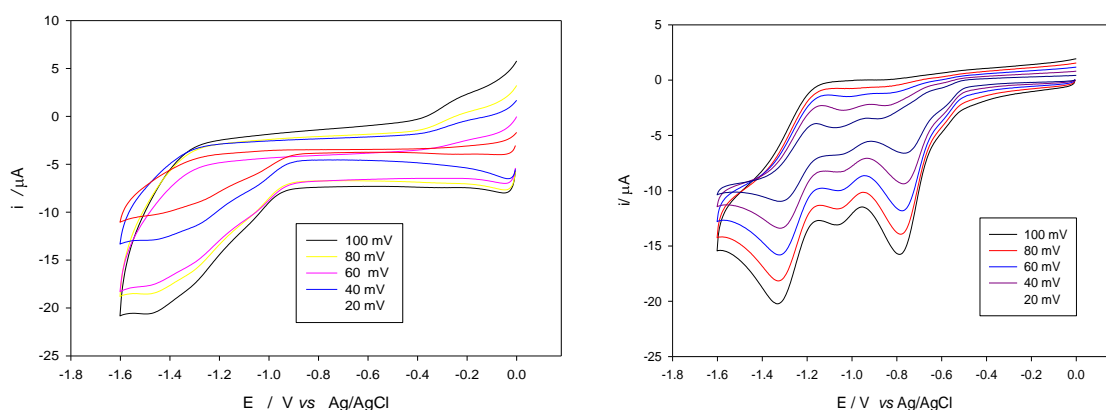


Figure 6. Cyclic voltammetry of 0.2 M $[\text{NBu}_4][\text{BF}_4]$ solution at carbon electrode with different scan rate under nitrogen of 2.5 mM DMF solutions $[\text{Fe}(\text{H}_2\text{-PLSC})\text{Cl}_2(\text{H}_2\text{O})]\text{Cl}$ (left) and $\text{Fe}(\text{H-PLTSC})(\text{PLTSC})\cdot 4\text{H}_2\text{O}$ (right).

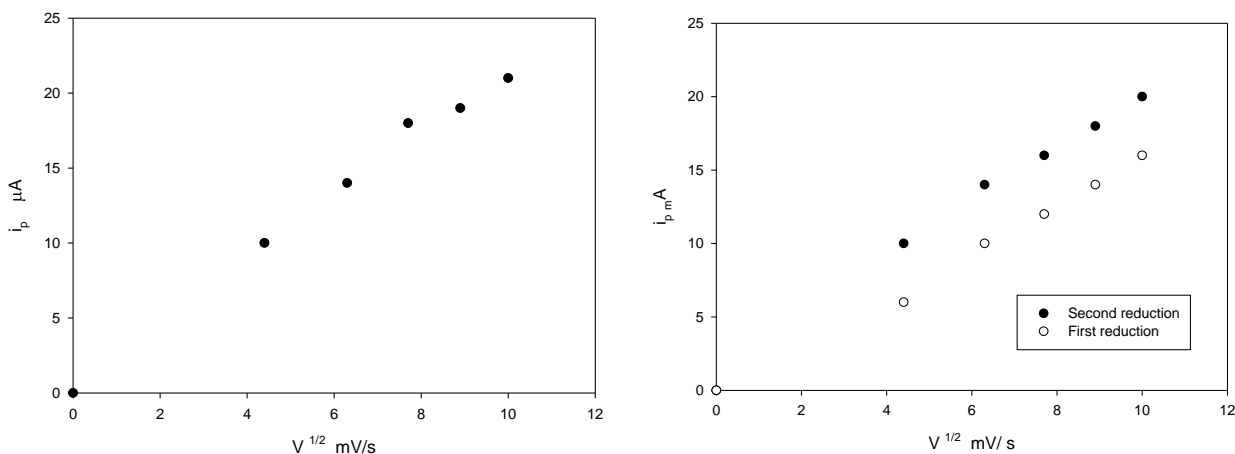


Figure 7. The dependence of square root of the scan-rate ($v^{1/2}$) on the peak current of $[\text{Fe}(\text{H}_2\text{-PLSC})\text{Cl}_2(\text{H}_2\text{O})]\text{Cl}$ (left) and $\text{Fe}(\text{H-PLTSC})(\text{PLTSC})\cdot 4\text{H}_2\text{O}$ (right)

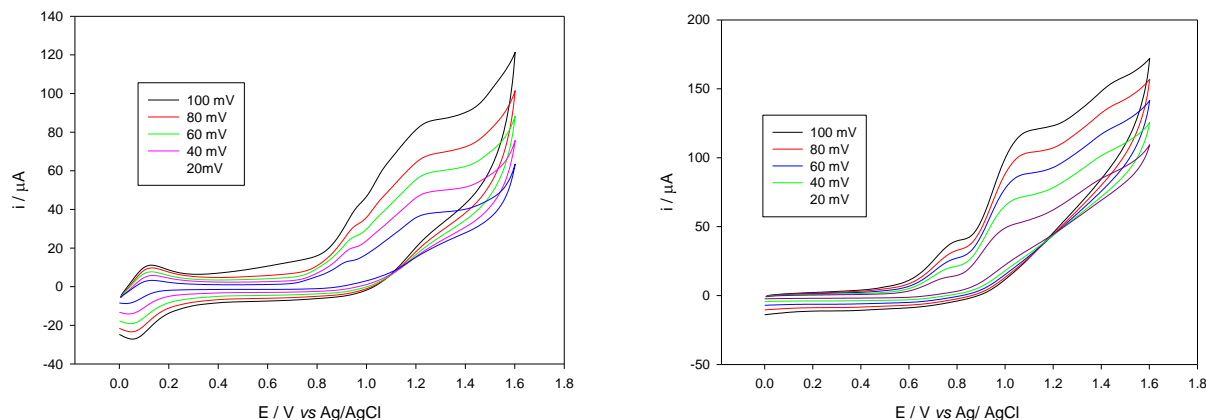


Figure 8. Cyclic voltammetry of 2.5 mM DMF solutions of $[\text{Fe}(\text{H}_2\text{-PLSC})\text{Cl}_2(\text{H}_2\text{O})]\text{Cl}$ (left) and $\text{Fe}(\text{H-PLTSC})(\text{PLTSC})\cdot 4\text{H}_2\text{O}$ (right) in 0.2 M $[\text{NBu}_4][\text{BF}_4]$ -DMF solution at carbon electrode with different scan rate under nitrogen

In fact, the addition of acetic acid (CH_3COOH) in the presence of the O-containing or S-containing complexes, initiated the proton reduction process at catalytic currents of -1.3 and -1.2 V vs Ag/AgCl which became irreversible with the concentration of acid. This is consistent with the electrocatalytic proton reduction (Figures 9 and 10). Comparing to the catalyst-free acetic acid (CH_3COOH) in 0.2 M $[\text{NBu}_4][\text{BF}_4]$ -DMF (control experiment) at vitreous carbon electrode (figure 4), we highlight redox potential E_p shifts about 550, 450 mV for $[\text{Fe}(\text{H}_2\text{-PLSC})\text{Cl}_2(\text{H}_2\text{O})]\text{Cl}$ or $\text{Fe}(\text{H-PLTSC})(\text{PLTSC})\cdot 4\text{H}_2\text{O}$, respectively.

Figure 9 shows the reduction cyclic voltammetry of $[\text{Fe}(\text{H}_2\text{-PLSC})\text{Cl}_2(\text{H}_2\text{O})]\text{Cl}$ where the highest electrocatalytic activities was observed in the presence of 10 equivalent of acetic acid with maximum current that was equal to 4.4 times comparing to the free-acid medium. This value increased to 5.8 times for the complex $\text{Fe}(\text{H-PLTSC-H})(\text{PLTSC})\cdot 4\text{H}_2\text{O}$ (Fig. 10).

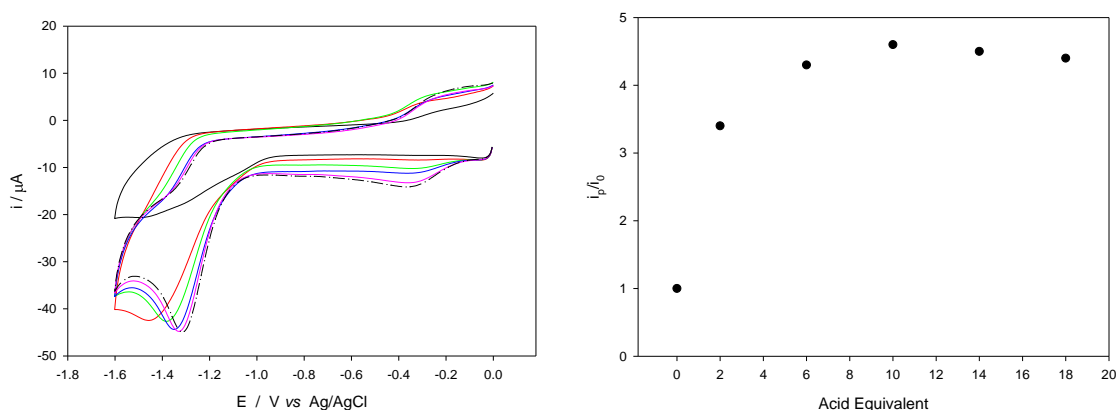


Figure 9. Cyclic voltammetry of 2.5 mM $[\text{Fe}(\text{PLSC})\text{Cl}_2(\text{H}_2\text{O})]\text{Cl}$ in DMF containing 0.1M $[\text{NBu}_4][\text{BF}_4]$, Rt. Scan rate 100 mVs^{-1} . in presence of 2eq , 6 eq , 10 eq , 14 eq , 18 eq , of acetic acid at carbon electrode electrode.

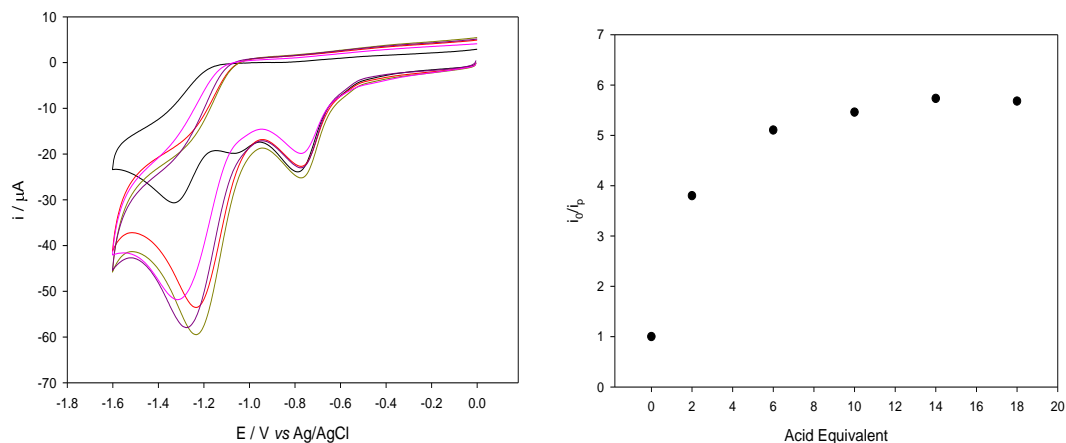


Figure 10. Cyclic voltammetry of 2.5 mM $\text{Fe}(\text{PLTSC-H})(\text{PLTSC-2H})\cdot 4\text{H}_2\text{O}$ in DMF containing 0.1M $[\text{NBu}_4][\text{BF}_4]$, Rt. Scan rate 100 mVs^{-1} . in presence of 2eq , 6 eq , 10 eq, 14 eq, 18 eq ,22 eq of acetic acid at carbon electrode.

In order to gather relevant information regarding the mechanism we compared the proton reduction activity of $\text{H}_2\text{-PLTSC}$ ligand and $\text{Fe}(\text{H-PLTSC})(\text{PLTSC})\cdot 4\text{H}_2\text{O}$ (Figure 11). Even though the complex was observed to be a more active electrocatalyst for the reduction of protons comparing to the free ligand, this observation clearly indicated that the hydrogen production process was initiated ligand protonation. In fact, according McNamara and co-workers [29], a distorted square planar nickel complex containing a bis-dithiocarbazate ligand exhibited a faradaic yield of 98% at an applied potential of $-1.8 \text{ V vs. Fc}^+/\text{Fc}$ in the presence of trifluoroacetic acid in acetonitrile. Additionally, a rinse test showed no catalytically active films formation on the electrode surface and based on the previously proposed mechanism of catalytic reaction we could postulate a mechanism for our system as shown in Scheme 1.

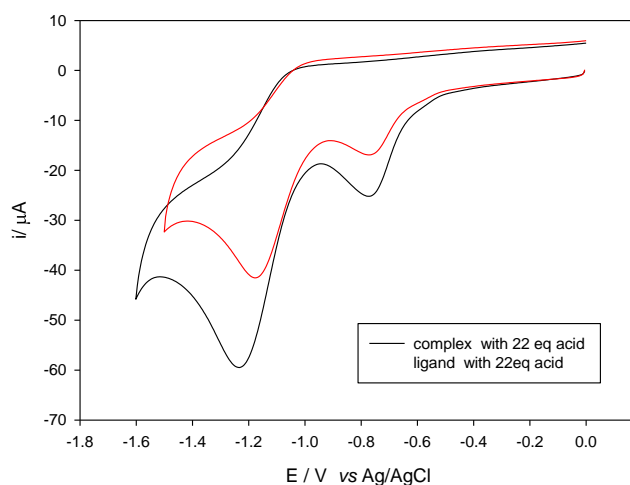
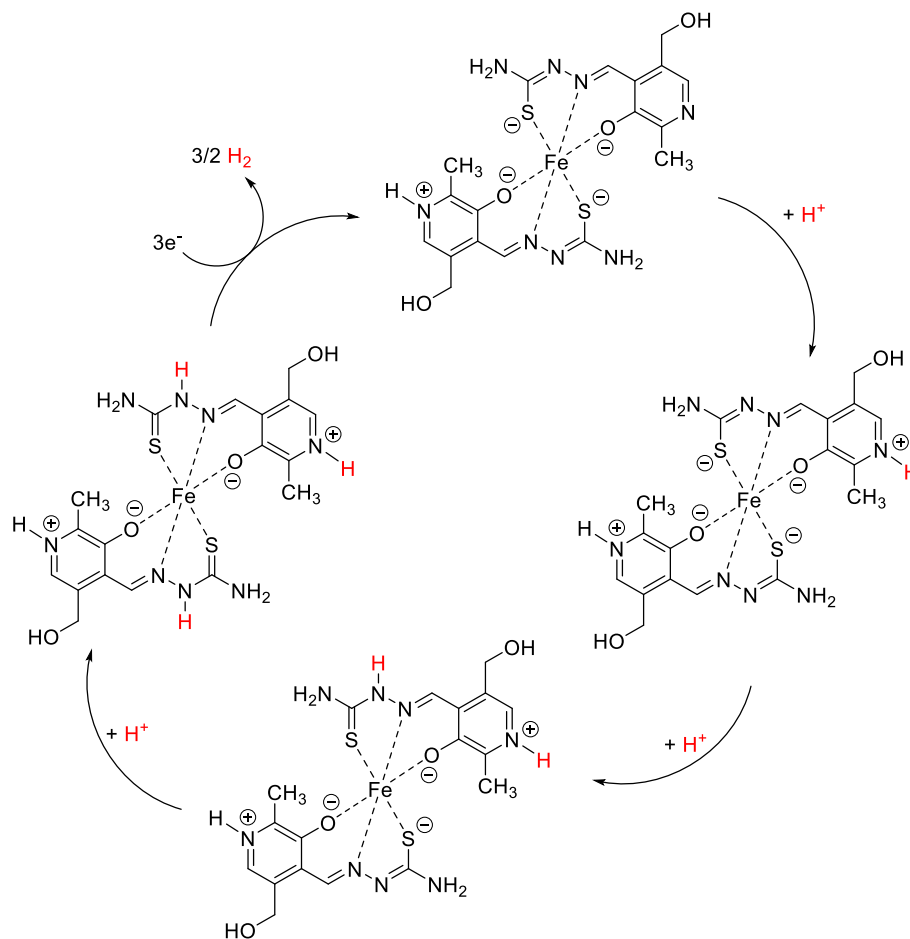


Figure 11. Cyclic voltammetry of 0.2 mM free ligand ($\text{H}_2\text{-PLTSC}$) and complex $\text{Fe}(\text{H-PLTSC})(\text{PLTSC})\cdot 4\text{H}_2\text{O}$ in DMF containing 0.1M $[\text{NBu}_4][\text{BF}_4]$, Rt. Scan rate 100 mVs^{-1} in presence of 22 eq acetic acid.

Having overview previous research [30] in the field of electrochemistry of ligands PLSC and PLTSC, we can assume the mechanism of hydrogen production.



Scheme 1. Proposed electrochemical generation of H₂ as catalyzed by complex [Fe(H-PLTSC)(PLTSC)]·4H₂O

In our case, we believe that complex [Fe(H-PLTSC)(PLTSC)] could accept three protons to form a new complex [Fe(H₂-PLTSC)₂]³⁺ in which both ligands would be in the neutral form followed by reductive release of 3/2 H₂ to re-generate the starting complex. This would be possible as the starting complex contains deprotonated ligands which would allow it to, under electrocatalytic conditions, accept additional protons followed by reduction to molecular hydrogen. The mechanism would also account for the observed difference in efficiency between [Fe(H₂-PLSC)Cl₂(H₂O)]Cl and Fe(H-PLTSC)(PLTSC)]·4H₂O. The former complex contains the ligand in its neutral form which does not provide any incentives for binding of protons. In the case of Fe(H-PLTSC)(PLTSC)]·4H₂O, the ligands are deprotonated so their electrochemical protonation (followed by reduction to produce molecular hydrogen) would be favorable in comparison to the H₂-PLSC-containing complex.

Furthermore, as both ligands H₂-PLSC and H₂-PLTSC appeared to be active in generation of molecular hydrogen these molecules could be viewed as new organocatalysts [31] adding to the fast-growing area of hydrogen generation by organic molecules [32,33, 34,35,36]. For example, 2,2'-

dipyridylamine was reported as organic molecular electrocatalyst for hydrogen evolution reaction in acidic electrolytes showing remarkable catalytic activity and performance durability in strongly acidic polymer electrolytes [35]. Hydrogen production from catalytic polyethylene terephthalate (PET) is another example of efficient usage of organocatalysis as this material was used for waste reforming reaction. This is quite significant as PET is one of the major products of plastic waste.[36]

The effects of H₂-PLSC, PLTSC, [Fe(PLSC)Cl₂ (H₂O)]Cl] ,and Fe(PLTSC-H)(PLTSC-2H)]·4H₂O on HER are compared with the previously reported complexes (Table 1).

The Table 1 shows the shifting of potential which significantly dependent on both of the type of complex and proton source. The ligands and complexes which used in this work shift the potential 400 – 600 mV. Similarly, other iron and cobalt complexes exhibited lower shift even tested using different sources of the protons.

Table 1. Comparing the effect of various complexes on HER

| Complex | Proton source | Potential of catalyst-free direct reduction (V) | Potential of reduction of acid in the presence of catalyst | Potential shifting | Condition | Ref. |
|--|----------------------|---|--|--------------------|--|---------------------|
| H ₂ -PLSC (ligand) | AcOH | -1.8 Ag/AgCl | -1.4 Ag/AgCl | 400 mV | [NBu ₄][BF ₄] –DMF | <i>Current work</i> |
| PLTSC (ligand) | AcOH | -1.8 Ag/AgCl | -1.20 Ag/AgCl | 600 mV | | |
| [Fe(PLSC)Cl ₂ (H ₂ O)]Cl] | AcOH | -1.8 Ag/AgCl | -1.3 Ag/AgCl | 500 mV | | |
| Fe(PLTSC-H)(PLTSC-2H)]·4H ₂ O | AcOH | -1.8 Ag/AgCl | -1.2 Ag/AgCl | 600 mV | | |
| [Ni(P ₄ N ₂)(CH ₃ CN)] ²⁺ | HOTf | 1.2 V Ag/AgNO ₃ | 1.2 Ag/AgNO ₃ | No shift | [NBu ₄]ClO ₄ –DMF | [37] |
| [Co ₂ L ₂ Cl ₃]Cl | Water | -1.40 V Ag/AgCl | -1.40 Ag/AgCl | No shift | phosphate buffer (pH 3.6 -7.0) | [38] |
| Co(TFPP) | AcOH | -1.81 Ag/AgNO ₃ | -1.45 Ag/AgNO ₃ | 360 mV | [NBu ₄]ClO ₄ –DMF | [39] |
| [Fe ₄ S ₄ (SPh) ₄] ⁻² | Ltd | -1.36 Ag/AgCl | -0.87 Ag/AgCl | 500 mV | [NBu ₄][BF ₄]–Toluene | [40] |
| Fe(PFTPP)Cl | TEA | -1.6 Ag/AgCl | -1.3 Ag/AgCl | 300 mV | [NBu ₄][BF ₄]–ACN | [41] |
| Mn(TPP)Cl | Et ₃ NHCl | -1.60 Ag/AgCl | -1.2 Ag/AgCl, | 400 mV | [NBu ₄][BF ₄]–CH ₃ CN | [42] |

ACN = Acetonitrile, AcOH = Acetic acid, DMF = Dimethylformamide, LTD = 2,6-lutidine, TEA = Triethylamine
Trifluoromethanesulfonic acid (HOTf)., triethylamine hydrochloride (Et₃NHCl)

4. CONCLUSION

This paper aimed to present the potential use of iron complexes based PLSC and PLTS ligands, as electrocatalysts for proton reduction into molecular hydrogen. The study of the electrocatalytic performance of these complexes was motivated by the observed activities of the uncoordinated ligands. In fact, comparing to the ligand-free solution, the redox potential specific to the reduction of the acetic acid proton E_p shifts about 350 mV and 550 mV to the more positive potentials, in the presence of PLSC

or PLTSC respectively. These results allow us to conclude that the use of proton deficient ligands is of great interest for proton reduction, especially, when attached to a metal. Therefore, high electrocatalytic activities of iron complexes based on PLSC and PLTSC towards hydrogen production by proton reduction were highlighted. Moreover, we can note that complexes based on deprotonated form (mono- or di-anionic form) of PLSC and PLTSC have better ability to produce hydrogen than those containing ligands in neutral form. Clearly, these results support the proposed mechanism involving the protonation of ligand followed the protonation of metal.

The conclusion is that proton deficiency, ie the presence of deprotonated atoms/ligands is a crucial condition for the formation of hydrogen.

Here we have the opportunity for a very bold statement, and it concerns the possibility that the ligands PLSC and PLTSC are can be viewed as new organocatalysts.

Also, It is possible conclude that complexes possessing a coordinated ligand in de-protonated form mono- or di-anionic form), will have a better ability to produce hydrogen, than complexes in which the PLSC or PLTSC ligand is coordinated in neutral form.

ACKNOWLEDGEMENT

This research has been funded by scientific research deanship at University of Hail- Kingdom of Saudi Arabia through project number RG-20072

References

1. N. S. Lewis and D. G. Nocera, *Proc. Natl. Acad. Sci of the United States of America*, 103 (2006) 15729-15735.
2. L. Yuan and J. Koo , *Biotechnol. Bioeng.*, 116 (2019) 3124 —3135.
3. W. Lubitz , H. Ogata , O. Rüdiger and E. Reijerse, *Chem. Rev.*, 114 (2014) 4081- 4148.
4. J. R. McCone, Marinescu , B. J. R. Brunshwig, B. S. Winkler and H. B. Gray , *Chem. Sci.*,5 (2014) 865 - 878.
5. I. Bhugun, D. Lexa and J. M. Savéant, *J. Am. Chem. Soc.*, 118 (1996) 3982 -3983.
6. Y. Xu and R. Xu , *Appl. Surf. Sci.*, 351 (2015) 779 -793.
7. H. Lei, H. Fang, Y. Han, W. Lai, X. Fu and R. Cao, *ACS Catal.*, 5 (2015), 5145 -5153.
8. B. D. Stubbert, J. C. Peters and H. B. Gray, *J. Am. Chem. Soc.*, 133 (2011) 18070 -18073.
9. P. Zhang, M. Wang, Y. Yang, D. Zheng, K. Han and L. Sun, *Chem. Commun.*, 50 (2014) 14153 - 14156.
10. J. W. Jurss, R. S. Khnayzer , J. A. Panetier , K. A. E. Roz , E. M. Nichols, M. Head-Gordon , J. R. Long, F. N. Castellano and C. J. Chang, *Chem. Sci.*,6 (2015) 4954 -4972.
11. H. Dobbek, L. Gremer, R. Kiefersauer, R. Huber and O. Meyer, *Proc. Natl. Acad. Sci. U. S. A.*, 99 (2002) 15971-15976.
12. J. M. Tunney, J. McMaster and C. D. Garner, *Comprehensive Coordination Chemistry II*, J. A. Mc Cleverty and T. J. Meyer, Elsevier–Pergamon, (2004) vol. 8, 459 Oxford, UK
13. R. Ramachandran, G. Prakash, S. Selvamurugan, P. Viswanathamurthi, J. G. Malecki, W. Linert and A. Gusev, *RSC Adv.*,5 (2015) 11405-11422.
14. S. Muthumari and R. Ramesh, *Chemistry Select.*, 3 (2018) 3036-3041.
15. B. Souza, L. Faustino, F. Prado, R. Sampaio, P. Maia, A. Machado and A. Patrocínio, *Dalton Trans.*, 49 (2020) 16368-16379
16. X. Jing, P. Wu, X. Liu, L. Yang, C. He and C. Duan, *New J. Chem.*, 39 (2015) 1051-1059.

17. M. Islam, D. Hossain, P. Mondal, K. Tuhina, A. Roy, S. Mondal and M. Mobarak, *Transition Metal Chemistry*, 36 (2011) 223-230.
18. P. Ranjan-Verma, S. Mandal, P. Gupta and B. Mukhopadhyay, *Tetrahedron Letters* 54 (2013) 4914-4917.
19. I. D. Kostas and B. R. Steele, *Catalysts*, 10 (2020) 1107-1147.
20. V. Jevtovic, Cu, Fe, Ni and V Complexes With Pyridoxal Semicarbazones: Lap Lambert Publication, book (2010) Saarbrücken, Germany.
21. V. Leovac, V. Jevtović, L. Jovanović and G. Bogdanović, *Journal of Serbian Chemical Society*, 70 (2005) 423-439.
22. V. Jevtovic, G. Pelosi, S. Ianeli, M. Leovac, R. Kovacevic and R. Kaisarevic, *Acta Chimica Slovenica*, 57 (2010) 363-369.
23. V. Jevtovic, D. Vidovic, *Acta Crystallographica*, E 66 (2010) m408-m409.
24. V. Jevtovic, D. Cvetkovic and D. Vidovic, *Journal of Iranian Chemical Society*, 8 (2011) 727-733.
25. D. Vidovic, D. Radulovic and V. Jevtovic, *Polyhedron*, 30 (2011) 16-21.
26. V. Jevtovic, *Research in Cancer and Tumor*, 3 (2014) 1-5.
27. R. Manikandan, P. Anitha, G. Prakash, P. Vijayan and P. Viswanathamurthi, *Polyhedron*, 81 (2014) 619-627.
28. R. Manikandan, P. Anitha, Periasamy Viswanathamurthi, Jan Grzegorz Maleck, *Polyhedron*, 119 (2016) 300-306.
29. C. F. Wise, D. Liu, K. J. Mayer, P. M. Crossland, C. L. Harley and W. R. McNamara, *Dalton Trans.*, 44 (2015) 14265—14271
30. Lj. Vojinović-Ješić, Lj. Jovanović, V. Leovac, M. Radanović, M. Rodić, B. Holló, K. Mészáros Szécsényi and S. Ivković, *Polyhedron*, 101 (2015) 196-205.
31. V. da Gama Oliveira, M. do Carmo Cardoso and L. da Silva Magalhães Forezi, *Catalysts* 8 (2018) 605-634.
32. S. Xiang and Bin Tan, *Nature Communications*, 11 (2020) 3786-3791.
33. A. Sinibaldi, V. Nori, A. Baschieri, F. Fini, A. Arcadi and A. Carlone, *Catalysts*, 9 (2019) 928-963.
34. I. Shaikh, *Journal of Catalysts*, (2014) Article ID 402860
35. L. Lin, H. T. Chung, U. Martinez, A. Baker, S. Maurya and P. Zelenay, *J Am Chem Soc.* (2019) <https://doi.org/10.26434/chemrxiv>,
36. W. Nabgan, B. Nabgan, T. Abdullah, N. Ngadi, A. Jalil, A. Nordin, N. Latif and N. Othman, *Catal. Sustain. Energy*, 7 (2020) 45–64.
37. Ling-Zhi Fu, Ling-Ling Zhou, Ling-Zhi Tang, Yun-Xiao Zhang, Shu-Zhong Zhan, *Journal of Power Sources* 280 (2015) 453-458
38. Dong-Xu Zhang, Hua-Hua, Wei-Hong Wen, Wei-Hong Wen, *Transit Met Chem* 42 (2017) 773–782
39. K. Alenezi, *Int. J. Electrochem. Sci.*, 12 (2017) 812–818.
40. A. Rana, B. Mondal, P. Sen, S. Dey and A. Dey, *Inorg. Chem.*, 56 (2017) 1783-1793
41. I. Bhugun, D. Lexa and J. Savéant, *J. Am. Chem. Soc.*, 118 (1996) 3982–3983
42. K. M. Alenezi *J. New Mat. Electrochem. Systems*, 20(2017) 043-047